

Synthesis and Catalytic Application of N-doped Carbons for Biomass Hydrolysis Jan. 2018 – Present

Supervisor: Dr. Hao MA and Prof. Fei QI, SJTU Combustion and Energy Research Group

1. Scalable Production of Nitrogen-doped Carbons (NCs)

Nitrogen-doped Carbons have extensive applications in energy storage and gas separation. The first research problem was how to synthesize NCs facilely, but with a high nitrogen content. I synthesized NCs with various cheap biomass precursors and altered the synthesis conditions, including air pretreatments and temperatures. The synthesis procedure is shown in Fig. 1.1. Scanning Electron Microscope (SEM) and Transmission electron microscopy (TEM) were adopted to characterize the morphology. The NCs particles are approximately spherical in shape, as shown in Fig. 1.2. X-ray photoelectron spectroscopy (XPS) was used to detect the distribution of nitrogen species on the surface, as shown in Fig. 1.3. The results of pyrolysis tests showed the relative elemental proportions in Table I, which indicated the highest nitrogen content in NC-700N-6. This work was reported at the 22nd International Symposium on Analytical and Applied Pyrolysis (Pyro2018) [1].



Fig. 1.1 Scalable Production Procedure

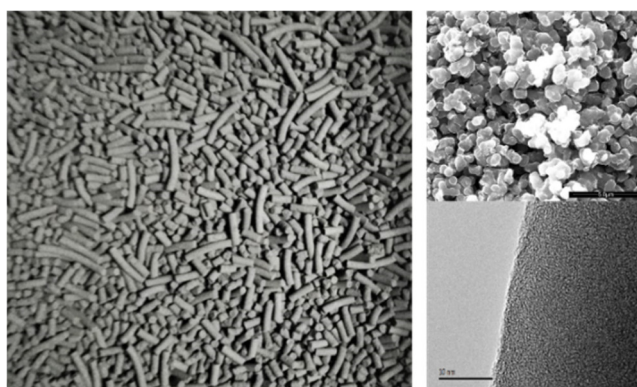
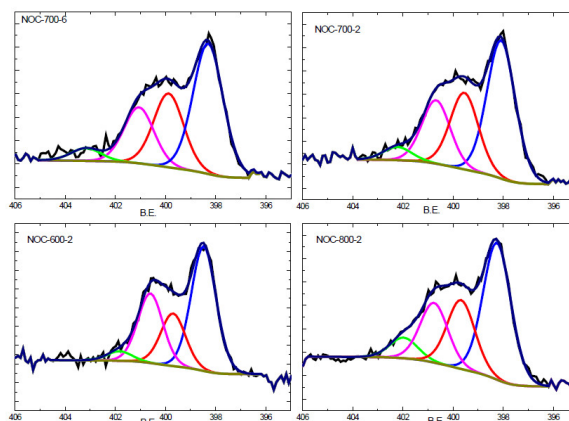


Fig. 1.2 Morphology of NCs



XPS of N1s (pyridinic, pyrrolic, quaternary and pyridinic N⁺-O⁻)

Fig. 1.3 Distribution of Nitrogen Species

Table I
Properties of NCs with different pyrolysis (* wt% from combustion analysis)

| Samples | Pretreatment in Ar | Pyrolysis in NH ₃ | BET SSA (m ² /g) | N % * | H % * | O % * |
|-----------|-----------------------|---------------------------------|--------------------------------|----------|----------|----------|
| OC-700-6 | 700°C for 6 h | none | 669 | 0 | 1.1 | 3.5 |
| NC-700N-6 | none | 700°C for 6 h | 681 | 13.5 | 1.2 | 6.5 |
| NC-700-2 | 350°C for 0.2 h | 700°C for 3 h | 623 | 11.1 | 1.0 | 5.0 |
| NC-700-6 | 350°C for 0.2 h | 700°C for 6 h | 698 | 12.3 | 1.1 | 4.6 |
| NC-600-2 | 350°C for 0.2 h | 800°C for 2 h | 506 | 5.9 | 2.5 | 7.5 |
| NC-600-6 | 350°C for 0.2 h | 600°C for 6 h | 584 | 7.0 | 2.2 | 6.9 |
| NC-800-2 | 350°C for 0.2 h | 800°C for 2 h | 720 | 10.9 | 0.9 | 4.9 |
| NC-800-6 | 350°C for 0.2 h | 800°C for 6 h | 803 | 10.5 | 0.8 | 2.8 |

2. N-Doped Carbon–Silica Composite Confined Pd Nanoparticles for Abatement of Methane Emission

Based on the preparation of NCs, I collaborated on another project to synthesize a Palladium-based catalyst for abatement of methane emission from automobiles. As a support, the as-synthesized NC can well disperse Pd nanoparticles and preserve part of active Pd nanoparticles (< 8 nm) with aging in severe conditions. The better dispersions of Pd in Pd/NC catalysts are shown in Fig. 1.4 and the size distributions are shown in Fig. 1.5.

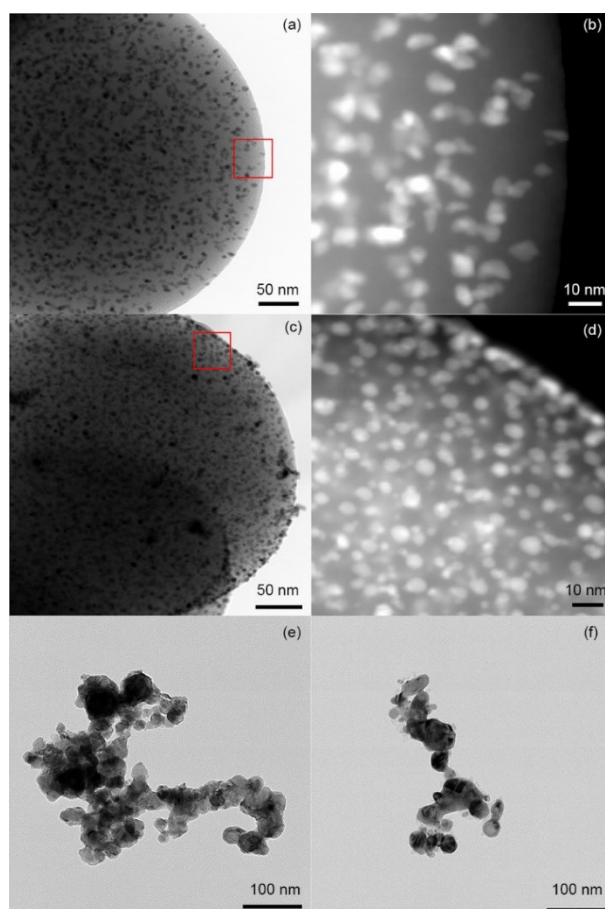


Fig. 1.4 TEM (a, c, e, f) and HAADF (b, d) micrographs of Pd loading supports with or without N-doping: (a, b) fresh Pd/NC; (c, d) fresh Pd/C; (e) Pd/NC and (f) Pd/C after catalytic test.

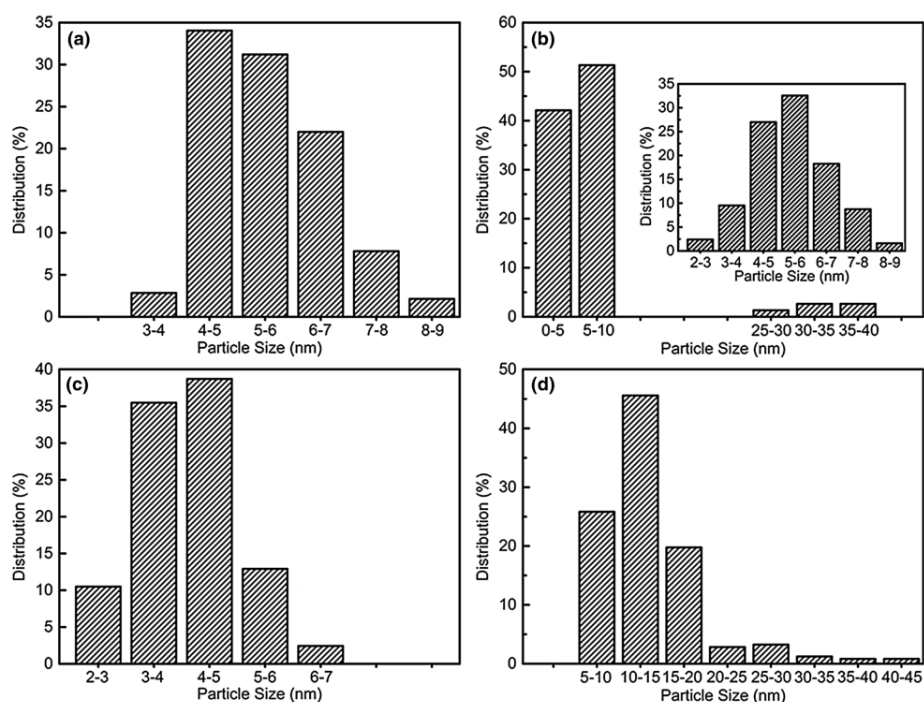


Fig. 1.5 The size distributions of Pd particles in fresh catalysts: (a) Pd/NC, (b) (Pd/NC)@SiO₂, (c) Pd/C, and (d) (Pd/C)@SiO₂

With a silica coating, the catalyst (Pd/NC)@SiO₂ performs stable and complete conversion of 5000 ppm of CH₄ to CO₂ and H₂O at 350°C, as shown in Fig 1.6. A second-authored article has been published in *Topics in Catalysis* [2] and future optimization will focus on the thermal stability of the support.

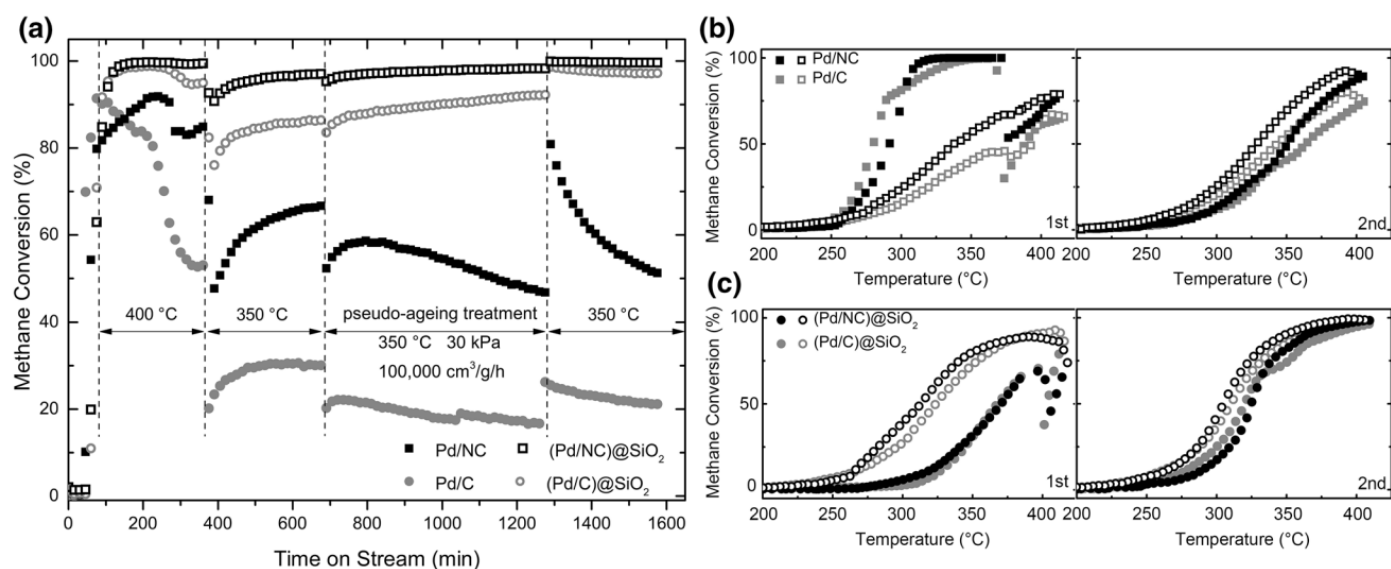


Fig. 1.6 Catalytic evaluation of (a) stability tests and (b, c) light-off curves of four catalysts: Pd/NC, Pd/C, (Pd/NC)@SiO₂, and (Pd/C)@SiO₂. Conditions: space velocity 40,000 cm³/g_{cat}/h at 10 kPa ga. Dense and hollowed symbols in (b) and (c) stand for heating-up and cooling-down, respectively.

3. Effective Methods for A Better Control of Nitrogen Species

Further research has been conducted to investigate effective methods for a better control of nitrogen species in NCs. Given that nitrogen doping can introduce more nitrogen onto furan-like five-membered rings to form pyrrolic-N (N-5), making NCs an acid-base catalyst, one problem was how to synthesize them facilely, yet

with a higher content of N-5. Hydrothermally synthesized carbons from aqueous glucose solution are selected as precursors. Inspired by the industrial synthesis procedure of pyrrole from furan with solid acid catalysts, I expected the addition of Lewis acid, such as alumina, would also increase the content of N-5. By altering the temperature and alumina ratio, I synthesized 15 catalysts. From the XPS results shown in Fig. 1.7, parts of these catalysts have shown a peak shift from pyridinic-N to pyrrolic-N, thus validating my perspective. Future optimization will focus on the selection of different Lewis acids, such as Zinc Chloride.

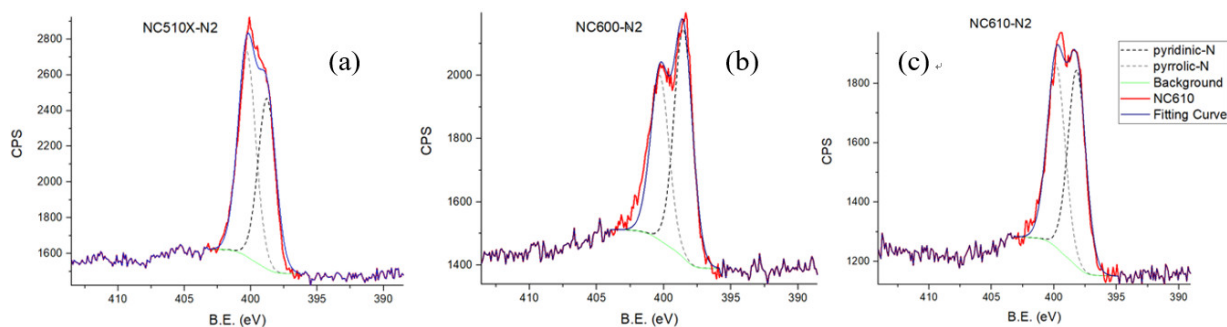


Fig. 1.7 XPS and curve fitting results of (a) NC510X, (b) NC600 and (c) NC610. NC510X means that after ammonification at 500°C with 10wt% doping of Aluminum, the sample was washed with aqua regia to remove alumina. NC600 indicates the ammonification temperature is 600°C with no Al. NC610 mean ammonification at 600°C with 10 wt% Al.

4. NCs as *Biomass-derive Catalysts for Catalytic Cellulose Hydrolysis*

Since the purpose of the research program was catalytic applications, I was curious about whether these biomass-derived catalysts could convert biomass, such as cellulose and xylose, to monomers. I selected a group of solid catalysts for the hydrolysis of cellobiose to produce glucose. With HPLC results indicating a poor catalytic performance, I am striving to increase the contact between catalysts and macro-molecules in two ways. One is to prepare Carbon Dots (CDs) through organic additives, such as ethylenediamine. The morphology of CDs is shown in Fig. 1.8. With theoretical calculations, I am now synthesizing smaller particles for catalytic experiments. The other attempt is to increase meso-porosity. Inspired by the TEM micrographs of aged Pd/NC catalysts, as shown in Fig. 1.9, I thought some oxygen radicals may be generated in the presence of Pd. Since it would be too expensive to use noble metals to increase meso-porosity, I doped three copper salts into NCs to catalyze oxidation reactions, in the hope that the generation of active oxygen radicals could produce more mesopores. With TGA, we analyzed the decomposition temperatures of three copper salts and designed the experiments, respectively. However, catalytic oxidation of Carbon Monoxide did not yield any obvious meso-porosity in NCs. We are now making attempts with Methane, similar to the process of methane abatement with Pd/NC.

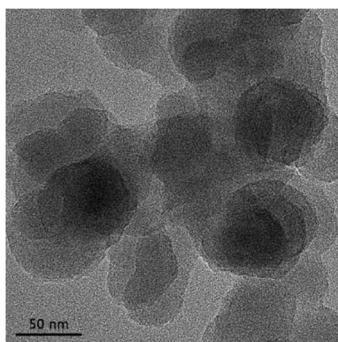


Fig. 1.8 Morphology of CDs Produced from Hydrothermal Treatment of Glucose with Ethylenediamine

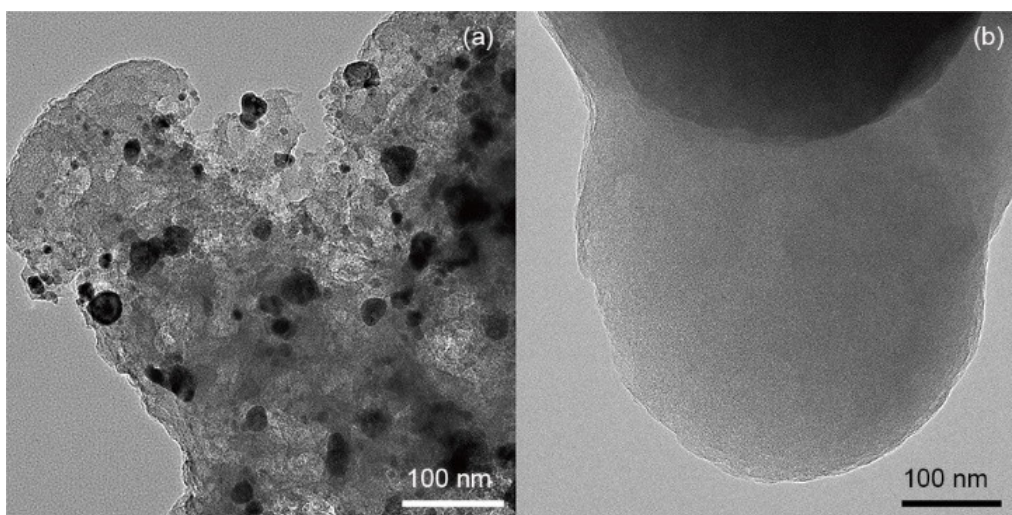


Fig. 1.9 TEM micrographs of aged (a) Pd/NC and (b) NC, with aging conditions: 400°C for 24 h with GHSV of 60,000 cm³/g_{cat}/h at 0.1 bar.

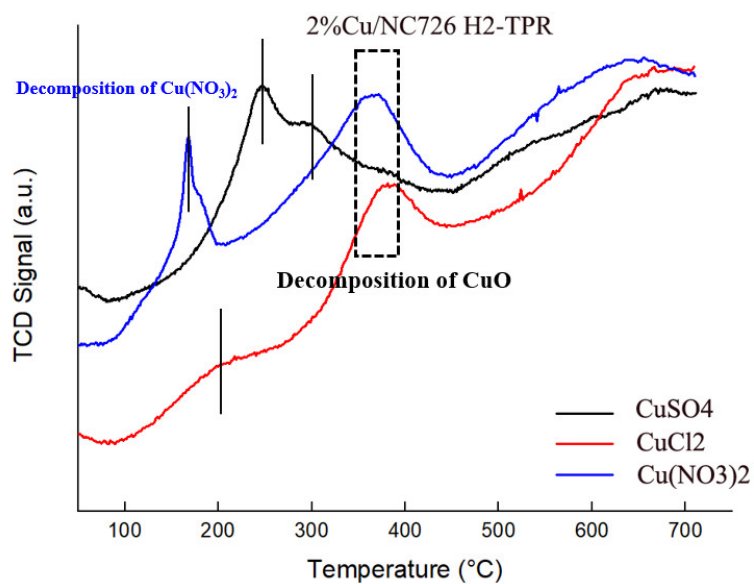


Fig. 1.10 H₂-TPR Profiles of Three Copper Salts: CuSO₄, CuCl₂ and Cu(NO₃)₂.

The research problem was the difficulty of building a reliable motion control system on a life-sized humanoid robot, due to the ultra-numerous DOF (29 DOFs) and the complicated structure. For the mechanical part, I implemented some modifications on STL files through reverse engineering and adopted additive manufacturing to realize the fast prototyping of a humanoid. The structure and DOF are shown in Fig. 2.1.

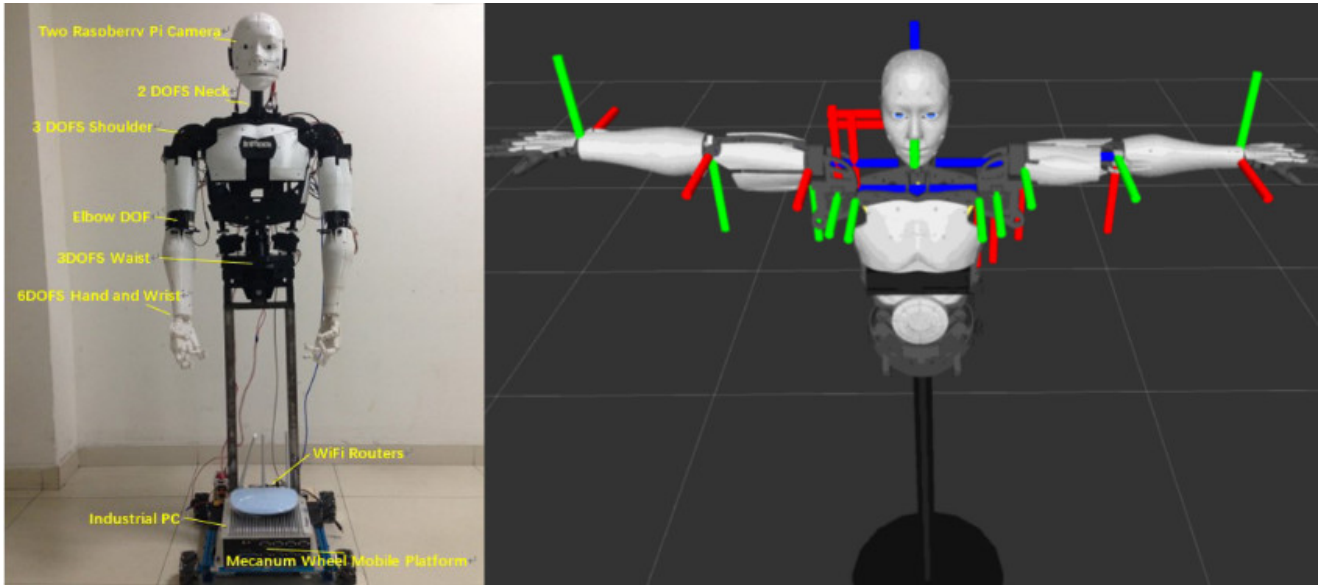


Fig. 2.1 Structure and DOF of Humanoid Robot

For the part of motion planning, I examined a wide range of parameters and IK solvers and finally selected the Kinematics and Dynamics Library (KDL). I also developed a 3D robot model for motion visualization (as shown in Fig. 1), a user-friendly interface for motion planning commands and an interface between controllers for data transmission. The first control scheme is shown in Fig. 2.2.

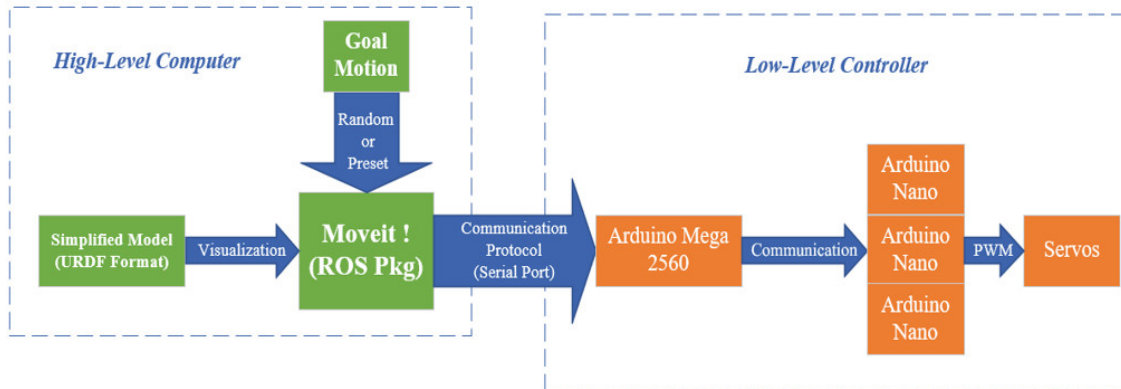


Fig. 2.2. 1st Control Scheme with Desired Motions

Based on the proposed control scheme, several fixed postures were stored in the robot to substitute traffic cops for traffic guidance through motion planning. The experimental results are shown in Fig. 2.3. Our system derived infinitely many possibilities for the robot applications and led to the first prize of senior undergraduate theses. The research work was later presented at the *IEEE International Conference on Advanced Robotics and Mechatronics (ICARM)* [3].

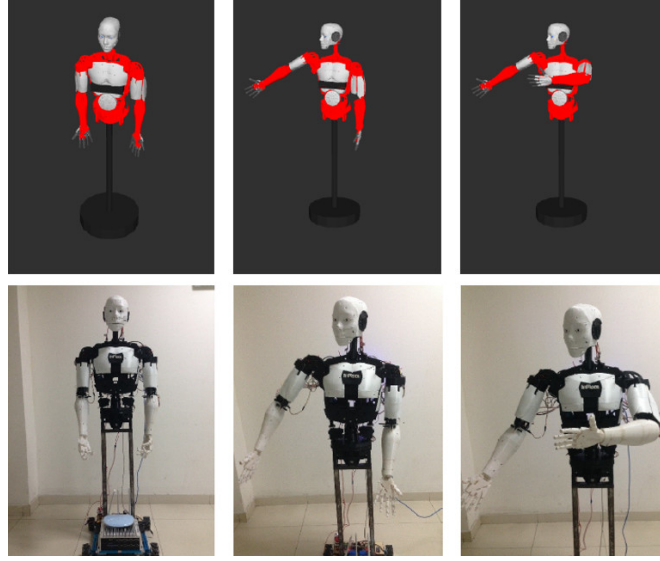


Fig. 2.3. Experimental Results of Motion Planning

Since the robot could only behave according to the several preset postures, the next step was to increase its flexibility. For the second control scheme, I adopted 32 Inertial Measurement Units (IMUs) to capture human motions. The technical problem we attempted to conquer was the motion conversion from the demonstrator with physiological constraints, to the humanoid with mechanical constraints, as shown in Fig. 2.4. Similar research works were summarized and for the sake of real-time performance, I eventually developed a real-time motion mapping algorithm. To further improve the accuracy of tele-manipulation, I proposed a natural teaching paradigm, where a live video stream was transferred from the humanoid to the demonstrator and the motion data were applied in the reverse direction, to form a human-in-the-loop control scheme. The part of perception and control is shown in Fig 2.5 and Fig 2.6, respectively.

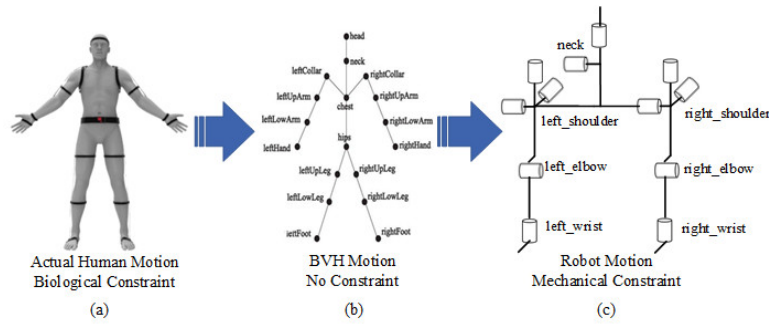


Fig. 2.4. Motion Conversion Problem

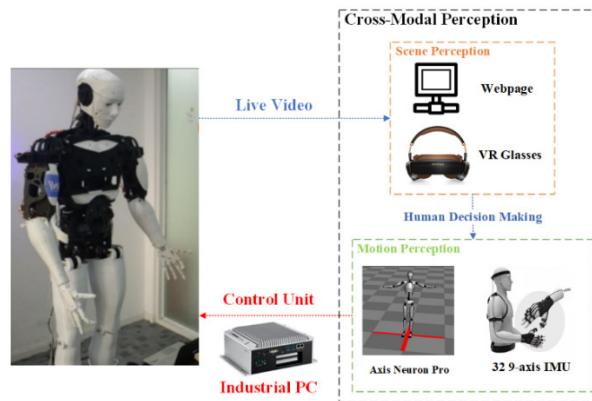


Fig. 2.5. 2nd Control Scheme (Perception Part)

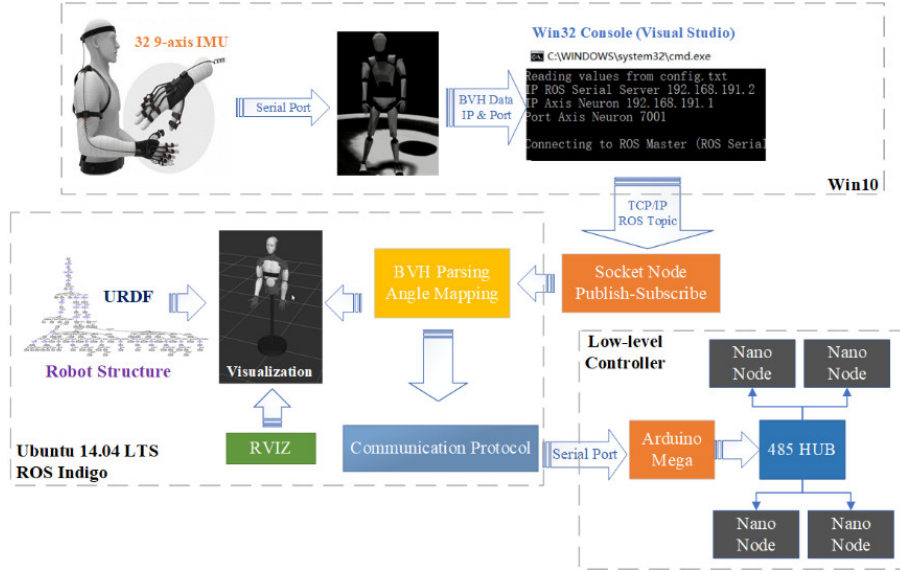


Fig. 2.6. 2nd Control Scheme (Control Part)

The proposed paradigm enabled me to contribute more to another graduation project with Best in Show Award and presented our work at *ICARM* again [4]. Besides traffic cops, we also expected to apply the natural teaching paradigm to industrial tasks. Hence, I submitted a first-authored research paper to *Industrial Robot* which has been accepted [5]. Later a third-authored letter was accepted by *Science China Information Sciences* [6]. The experimental results of motion imitation and natural teaching are shown in Fig. 2.7 and Fig. 2.8, respectively. In the future, I will replace wearable sensors with 2D pose estimation methods and establish connections between motion and scene information with machine learning methods, to further enhance robotic intelligence.

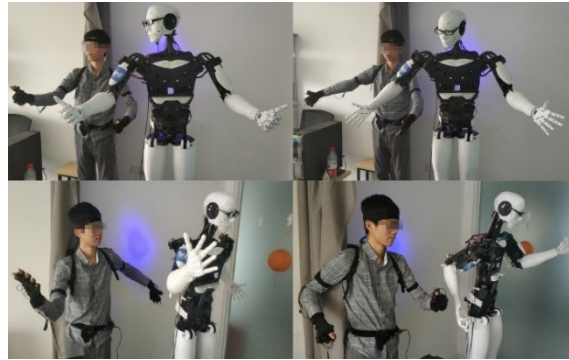


Fig. 2.7. Experimental Results of Motion Imitation



Fig. 2.8. Experimental Results of Natural Teaching

**Videos can be seen on my website (<http://wenbinxu.com/research/humanoid>)*

Reference

- [1] **W. B. Xu**, C. J. Liu, C. Q. Zhou, Z. Y. Zhou, H. Mao*, "Scalable Production of Nitrogen-doped Carbons by Pyrolysis of Biomass-derived Carbons in NH₃ Gas," 22nd International Symposium on Analytical and Applied Pyrolysis, Kyoto, Japan, 2018. **Conference Abstract**
- [2] C. Q. Zhou, **W. B. Xu**, C. J. Liu, X. M. Chen, Z. Y. Zhou, H. Mao*, F. Qi, N-doped Carbon-Silica Composite Confined Pd Nanoparticles for Abatement of Methane Emission from Automobiles, *Topics in Catalysis* 2018, 10.1007/s11244-018-1099-7
- [3] L. Gong et al., "Real-time human-in-the-loop remote control for a life-size traffic police robot with multiple augmented reality aided display terminals," 2017 2nd International Conference on Advanced Robotics and Mechatronics (ICARM), Hefei, 2017, pp. 420-425.
- [4] **W. B. Xu**, X. D. Li, W. D. Xu, L. Gong*, et al., "Human-robot Interaction Oriented Human-in-the-loop Real-time Motion Imitation on a Humanoid Tri-Co Robot," 3rd International Conference on Advanced Robotics and Mechatronics (ICARM), NUS, Singapore, 2018. **Oral Presentation | To Appear**
- [5] **W. B. Xu**, X. D. Li, L. Gong*, Y. X. Huang, et al., "Natural Teaching for Humanoid Robot via Human-in-the-loop Scene-motion Cross-modal Perception," *Industrial Robot*. **Accepted**
- [6] L. Gong*, X. D. Li, W. B. Xu, B. H. Chen, Z. L. Zhao, Y. X. Huang, C. L. Liu, Naturally Teaching a Humanoid Tri-Co Robot in a Real-time Scenario from First Person View, *Science China Information Sciences*. **Accepted**